Pulse Responses in the Dispersion Media

Ryosuke Ozaki[a)], Tomohiro Yanaka, Naoya Sugizaki, and Tsuneki Yamasaki[b)]
Department of Electrical Engineering, College of Science and Technology
Nihon University
Tokyo, Japan
a)ozaki@ele.cst.nihon-u.ac.jp, b)yamasaki@ele.cst.nihon-u.ac.jp

***Abstract*—In this paper, we propose a method for deciding the parameters to satisfy the experiment values, and also checked the effectiveness of this method based on Kramers-Kronig relation. In our proposed method, we are expressed as matrix the Sellmeier formula, and are solved the simultaneous equation until the satisfied experiment curve. Numerical results are given by the influence of pulse responses utilizing the fast inversion of Laplace transform (FILT)**

***Keywords*—fast inversion of Laplace transform; pulse responses; dispersion media;**

I. Introduction

Recently, the inverse scattering problem of electromagnetic waves has been of interest in many areas of remote sensing and imaging technology. In particular, the ground penetrating rader[1]-[3] is known as technology which can investigate the geometry in the soil. From the humanitarian support and land mine removal activity, these researches are widely performed in the world. Then, we are required to examine without destroying the target object buried in the soil. Therefore, it is very important to investigate the wave reflected from the scatterer such as target objects.

In this paper, we analyze the pulse responses of the structure buried the perfect conductor in the dispersion medium by using the experiment value of the dielectric constant in the 1.2g/cm^3 equivalent dry density of gray San Antonio clay loam[4]. However, in order to analyze the pulse responses with high accuracy, it is necessary to uniformly treat the complex dielectric constants of the dispersion media exactly. Though it is analyzed the inverse scattering problem such as buried mine-like target object by utilizing the FDTD method and various numerical techniques[1,3], it is not given the complex dielectric constants with a function of frequency in detailed. And so, we are employed the Sellmeier's formula[5] as a permittivity of dispersion media. But, it was difficult to determine the parameters including the above formula. In the purpose of this paper, we propose a method for deciding the parameters to satisfy the experiment values[4]. In our proposed method, we are expressed as matrix the Sellmeier's formula and orientational polarization, and are solved the simultaneous equation until the satisfied the experiments values, and also have checked effectiveness of this method based on Kramers-Kronig relation.

Numerical results are given for the influence of pulse responses using the medium constants which can be found by proposed method. Also, numerical technique of pulse responses is employed the fast inversion of Laplace transform (FILT)[8,9].

II. Method of Analysis

We consider the two dispersion media embedded with the perfect conductor at $x = d_1 + d_2$ as shown in Fig.1. The structure shown in the figure is uniform in the z-direction.

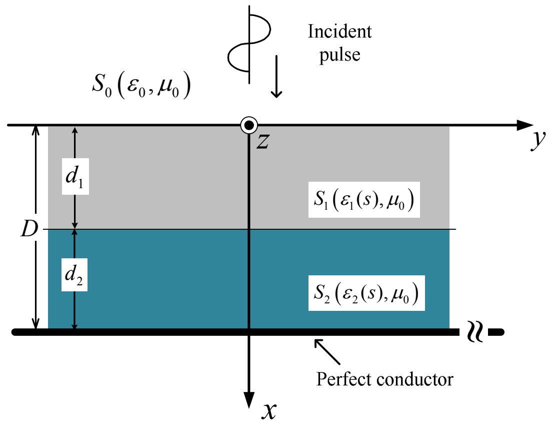

Fig.1 Structure and Coordinate system

The dielectric constants of regions S_0, S_1, and S_2 are defined by ε_0, $\varepsilon_1(s)$, and $\varepsilon_2(s)$, respectively. The permeability is assumed to be μ_0 in all regions. The waveform of incident pulse at $x = 0$ is assumed to be sine pulse and it can be expressed as[10]

$$e_0^{(i)}(t) = [u(t) - u(t - t_w)]\sin\{2\pi t/t_w\}, \tag{1}$$

where t_w is pulse width and $u(t)$ is a unit step function.

To analyze the complex frequency domain, image function $E_0^{(i)}(s)$ of Eq.(1) can be expressed as [10]

$$E_0^{(i)}(s) = \frac{(2\pi/t_w)}{s^2 + (2\pi/t_w)^2}(1 - e^{-st_w}). \tag{2}$$

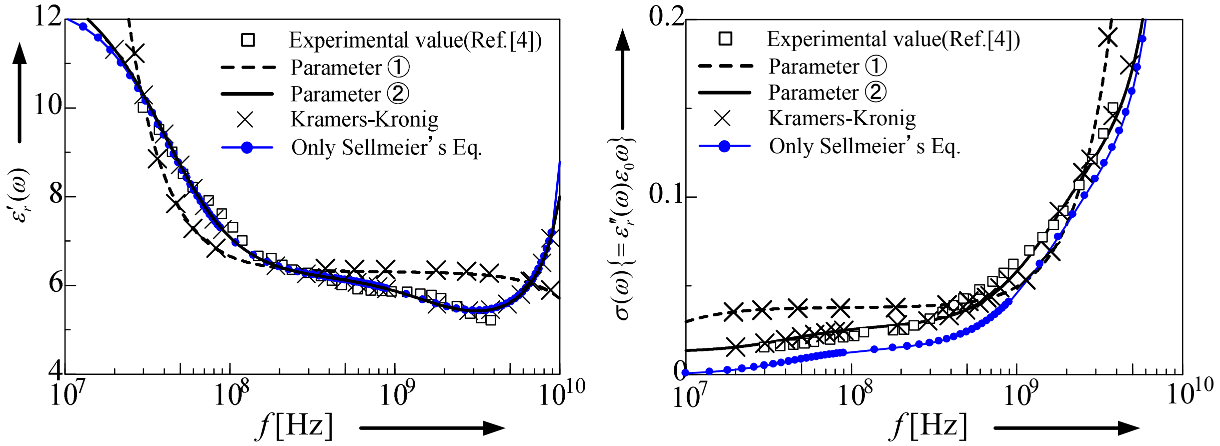

(a) The real part $\varepsilon_r'(\omega)$ (b) The imaginary part $\sigma(\omega)\{=\varepsilon_r''(\omega)\varepsilon_0\omega\}$

Fig.2 Comparison of complex dielectric constants for parameters ① and ②.

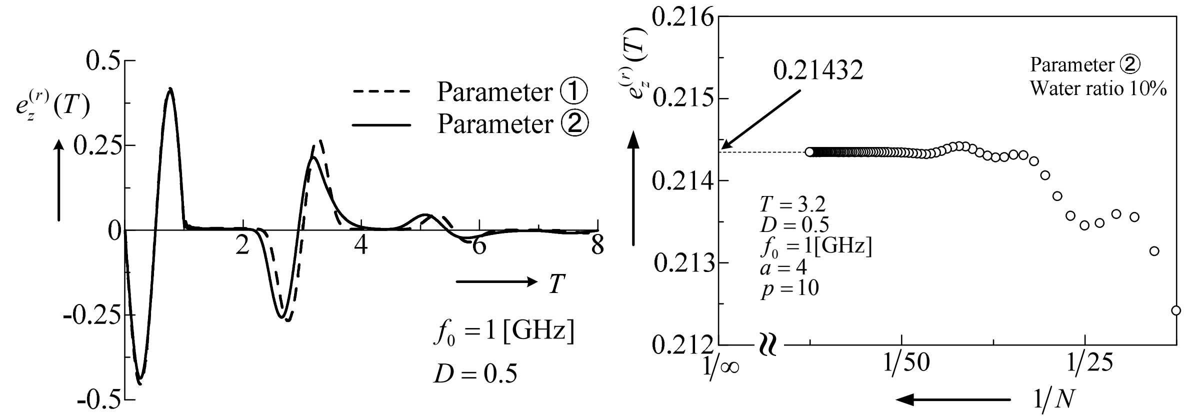

(a) Pulse responses for parameters ① and ② (b) Convergence of $1/N$ for parameter ②

Fig.3 Pulse responses and convergence of the FILT for the truncation mode number $1/N$.

The electric fields in the regions $S_0(x \le 0)$, $S_1(0 < x \le d_1)$, and $S_2(d_1 < x \le d_2)$ are given by

$$E_z^{(0)}(s) = E_0^{(i)}(s)e^{-\hat{k}_0 x} + E_z^{(r)}(s)e^{\hat{k}_0 x}, \quad (3)$$

$$E_z^{(1)}(s) = A_1 e^{-\hat{k}_1 x} + B_1 e^{\hat{k}_1 x}, \quad (4)$$

$$E_z^{(2)}(s) = A_2 e^{-\hat{k}_2 x} + B_2 e^{\hat{k}_2 x}, \quad (5)$$

$$\hat{k}_0 \triangleq s/c,\ \hat{k}_1 \triangleq \hat{k}_0\sqrt{\varepsilon_1(s)/\varepsilon_0},\ \hat{k}_2 \triangleq \hat{k}_0\sqrt{\varepsilon_2(s)/\varepsilon_0}, \quad (6)$$

where $\hat{k}_0$, $\hat{k}_1$, and $\hat{k}_2$ are the wave number, and the propagation constants in the x-direction of regions S_0, S_1 and S_2 . From the boundary conditions at $x = 0$, $x = d_1$, and $x = d_1 + d_2$, we obtain the reflected waves as the following equation:

$$E_z^{(r)}(s) = -\frac{C_1(s)e^{-2\hat{k}_2(d_2-d_1)} - \widetilde{R}_{23}e^{-2\hat{k}_2 d_1} - \widetilde{R}_{12}}{1 + \widetilde{R}_{12}\widetilde{R}_{23}e^{-2\hat{k}_2 d_1} - C_2(s)e^{-2\hat{k}_2(d_2-d_1)}} E_0^{(i)}(s), \quad (7)$$

where $C_1(s) \triangleq e^{-2\hat{k}_1 d_1} + \widetilde{R}_{12}\widetilde{R}_{23}$, $C_2(s) \triangleq \widetilde{R}_{23} + \widetilde{R}_{12}e^{-2\hat{k}_1 d_1}$

$\widetilde{R}_{12} \triangleq [1-\sqrt{\varepsilon_1(s)}]/[1+\sqrt{\varepsilon_1(s)}]$, $\widetilde{R}_{23} \triangleq [1-\sqrt{\varepsilon_2(s)}]/[1+\sqrt{\varepsilon_2(s)}]$.

Here, dielectric constant of dispersion media $\varepsilon_m(s)$ is expressed as Sellmeier's equation and orientational polarization considering the moisture [10].

$$\frac{\varepsilon_m(s)}{\varepsilon_0} = 1 + \sum_{i=1}^{3}\frac{q_i^2}{s^2 + g_{i,l}s + \Omega_{i,l}^2} + \frac{\tau_0}{1 + s\tau_l},\ (m = 1, 2). \quad (8)$$

The parameters of Eq.(8) are $(q_i, g_{i,l}, \Omega_{i,l})_{i=1,3}, (\tau_0, \tau_l)$.

Substituting $s = j\omega$ into Eq.(8), we get the complex dielectric constants as follows[10]:

$$\varepsilon_m(j\omega)/\varepsilon_0 \triangleq \varepsilon_r'(\omega) - j\varepsilon_r''(\omega), \quad (9)$$

$$\varepsilon_r'(\omega) \triangleq 1 + \sum_{i=1}^{3}\frac{q_i^2(\Omega_{i,l}^2 - \omega^2)}{(\Omega_{i,l}^2 - \omega^2)^2 + (\omega g_{i,l})^2} + \frac{\tau_0}{1 + (\omega\tau_l)^2}, \quad (10)$$

$$\varepsilon_r''(\omega) \triangleq \frac{\sigma(\omega)}{\omega\varepsilon_0} = \sum_{i=1}^{3}\frac{q_i^2(\omega g_{i,l})}{(\Omega_{i,l}^2 - \omega^2)^2 + (\omega g_{i,l})^2} + \frac{\tau_0(\omega\tau_l)}{1 + (\omega\tau_l)^2}, \quad (11)$$

where the real and imaginary parts of complex dielectric constants are given by Eqs.(10) and (11).

In the case of real part, we are obtained the parameters by the following procedure [10].

(1)First, we can be rewritten by matrix representation in Eq.(10) as following equation:

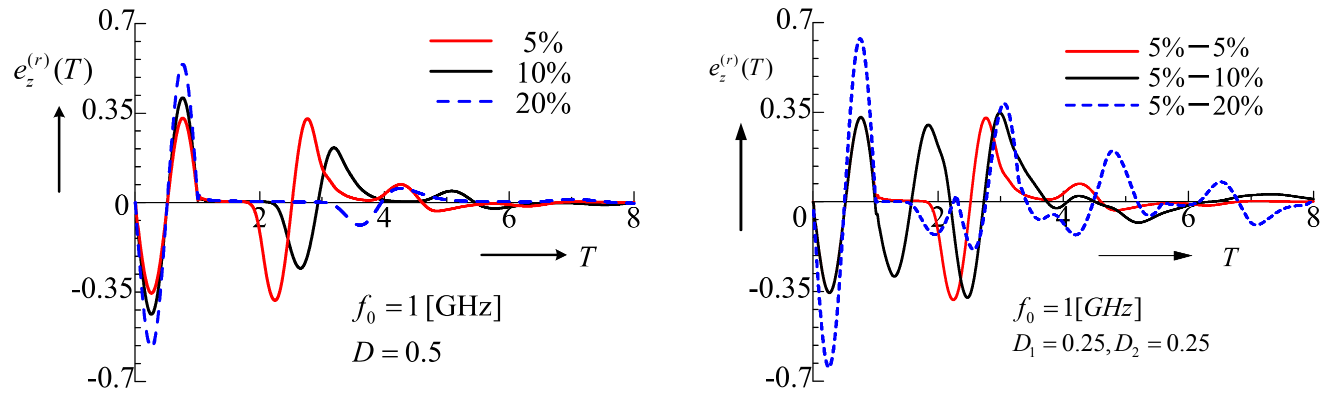

(a) $\varepsilon_1(s) = \varepsilon_2(s)$ (b) $\varepsilon_1(s) \neq \varepsilon_2(s)$

Fig.4 Pulse responses for condition of center frequency $f_0 = 1$ [GHz]

$$\mathbf{A}^{(l)}\mathbf{x}_0^{(l)} = \mathbf{B}, \tag{12}$$

where superscripts (l) indicate the iteration number of computing,

$$\mathbf{A}^{(l)} \triangleq \begin{bmatrix} \dfrac{(\Omega_{i,l}^2 - \omega_1^2)}{(\Omega_{i,l}^2 - \omega_1^2)^2 + (\omega_1 g_{i,l})^2} & \cdots & \dfrac{1}{1 + (\omega_1 \tau_l)^2} \\ \vdots & \ddots & \vdots \end{bmatrix},$$

$\mathbf{x} = [q_1^2, q_2^2, q_3^2, \tau_0]^T$, $\mathbf{B} \triangleq [b_1, b_2, b_3, b_4]^T$, T: transpose.

Matrix $\mathbf{A}^{(l)}$ is 4×4 coefficients matrix except parameters q_i^2 and τ_0, matrix $\mathbf{B}$ is experiment value against frequency ω. We have solved the simultaneous equation by using both the chosen parameters $(g_{i,l}, \Omega_{i,l})_{i=1\sim3}$, τ_l and $\mathbf{B}$ of arbitrary four points ω. In numerical analysis, we choose four sampling points in the frequency range of between 30MHz and 3840MHz given by the reference [4]. In fact, we have chosen the frequency four points at $f_1 = 30$[MHz], $f_2 = 120$[MHz], $f_3 = 960$[MHz], and $f_4 = 3840$[MHz][10].

(2)Second, we are calculated Eqs.(10) and (11) for real and imaginary parts by using the parameters obtained in above process. The next is found the errors ρ between both experiment and calculated values by using parameters obtained in the four points of real and imaginary parts corresponding to the frequency of matrix $\mathbf{B}$. If the result cannot be satisfied $|\rho| \leq 10^{-4}$, the elements of coefficients matrix $\mathbf{A}$ is changed by following equation:

$$\Omega_{i,l+1} \to \Omega_{i,l} + \Delta\Omega,\ g_{i,l+1} \to g_{i,l} + \Delta g\ ,\ \tau_{l+1} \to \tau_l + \Delta\tau\,. \tag{13}$$

Here, values of changing parameters ($\Delta\Omega, \Delta g$, $\Delta\tau$) are added to 10^{-3} order.

Then, it is solved a simultaneous equation again.

(3)Third, if the condition $|\rho| \leq 10^{-4}$ can be satisfied, we are performed for both real and imaginary parts as following condition in the middle three points of four points[10]:

$$\frac{d\varepsilon_r'(\omega)}{d\omega} < 0,\ \frac{d\sigma(\omega)}{d\omega} > 0\,. \tag{14}$$

If the results of an above condition cannot be satisfied, we return to procedure (1). If it is satisfied Eq.(14), next is progress.

(4)Finally, K. K. relation is employed as a check of the results obtained from these procedures. K. K. relation[7] is given by following equations:

$$\varepsilon_r'(\omega) \triangleq 1 + \frac{2}{\pi}\int_0^\infty \frac{\alpha\varepsilon_r''(\alpha)}{\alpha^2 - \omega^2} d\alpha\,, \tag{15}$$

$$\varepsilon_r''(\omega) \triangleq \frac{2\omega}{\pi}\int_0^\infty \frac{\varepsilon_r'(\beta)}{\beta^2 - \omega^2} d\beta\,. \tag{16}$$

In particular, we checked the influence for upper limit L of integration range and its frequency characteristics curve by utilizing the K. K. relation, and it has estimated whether real part to imaginary part is satisfied. These analyses are evaluated by using the numerical integral. In the numerical analysis, upper limit of integral range is truncated by L to be determined from convergence of integrand. If the results can be satisfied to experiment curve, we can be obtained the parameters for dispersion medium. In fact, the results of soil moisture with a water ratio of 10% found from in above procedure are as follows:

The electric field $E_z^{(r)}(s)$ using these parameters is transformed into the normalized time domain by utilizing the FILT[8,9].

$$\begin{aligned} e_z^{(r)}(T) &\triangleq \frac{1}{2\pi j}\int_{\gamma - j\infty}^{\gamma + j\infty} E_z^{(r)}(S) e^{ST}\, dS, \\ &= \frac{e^a}{T}\left(\sum_{n=1}^{N-1} F_n - 2^{-(p+1)}\sum_{q=0}^{p} A_{pq}F_{N+q}\right), \end{aligned} \tag{17}$$

where

$$F_n \triangleq (-1)^n \operatorname{Im}\left\{E_z^{(r)}\left(\frac{a + j(n-0.5)\pi}{T}\right)\right\}, \tag{18}$$

$$A_{pp} = 1,\quad A_{pq-1} \triangleq A_{pq} + \frac{(p+1)!}{q!(p+1-q)!}\,. \tag{19}$$

N is truncation mode number of the FILT, p is the number of terms in the Euler transformation, S is normalized complex frequency, and T is normalized time. We evaluate Eq.(17) to transform the reflective pulse responses in the time domain.

III. NUMERICAL RESULTS

Figures 2(a) and (b) show frequency characteristics for complex dielectric constants as the condition of San Antonio soil moisture with water ratio 10%. In this figure 2, the square plots (□) show experiment value in the San Antonio soil moisture with water ratio 10%, dashed line (– – –) is the result of parameter ① which is found by average of experiment value, black solid line is the result of parameter ② which is found by proposed method, and it is shown that the results of plotted (×) are calculated utilizing the K. K. relation which is truncated by $L(=2\pi\times10^{11})$. In addition, we are shown the results of only Sellmeier's equation by plotted blue line. From the Fig.2, we can see the following features:

(1)The results can be see the good agreement for between parameter ② and experiment value.

(2)The results of K. K. relation and parameters ① and ② can be seen clearly the good agreement.

(3)As the results of only Sellmeier equation, we can see the good agreement for experiment value in the real part. However, we can see an influence of orientational polarization in the imaginary part.

Therefore, in order to investigate the effects of parameters ① and ②, next we will be investigated the influence of parameters ① and ② by the pulse responses.

Figure 3(a) shows the pulse responses for parameters ① and ② as a condition of fixed normalized distance $D(\triangleq d/(ct_w)=d/\lambda_0)=0.5$ and $f_0=1[\mathrm{GHz}]$. From the Fig.3(a), we can see the following features:

(1)The initial pulse response at the $0<T\le1$ is almost same as for both parameters ① and ②. Since it is the response from the soil surface, we cannot see the influence of dispersion media.

(2)The response of $T\ge2$ is reflection from the perfect conductor. The influence of parameters can see clearly that it appear at both the amplitude and phase. In order to investigate the difference of parameter, next Fig.3(b) shows the convergence of $e_z^{(r)}(T)$ versus $1/N$ for fixed $T=3.2$. From this Fig.3(b), the relative error of $e_z^{(r)}(T)$ to the extrapolated true value are less than about 1% when we computed with $N=50$ and $p=10$.

Therefore, we can see that difference of the response for both parameters ① and ② as shown in Fig.3(a) is obtained by the effect of complex dielectric constants. We also obtained the dispersion medium parameters of the soil moisture 5% and 20% using the proposed method.

Figures 4(a) shows the pulse responses for various dispersion media with soil moisture 5%, 10%, and 20% as a condition of center frequency $f_0=1$ [GHz] and dispersion medium $\varepsilon_1(s)=\varepsilon_2(s)$ and $d_1=d_2$. From this figure, we can see the following features:

(1)The reflection responses ($T<1$) from the soil surface are obtained the difference of amplitude. As this reason, we can consider as the influence of equivalent permittivity of dispersion media by a real part.

(2)The reflection responses ($T\ge1.5$) from the perfect conductor can see clearly that it is difference by the amplitude and phase. As a reason of these results, we can consider that the difference appears by the influence of the real part at the delay time. On the other hand, we can understand that the amplitude is difference by the influence of the imaginary part.

Figure 4(b) shows the result of pulse responses for two dispersion media as a condition of $f_0=1$ [GHz] and $D_1=D_2=0.25$. The black solid line is the result of 5% as shown in Fig.5(a), the red dashed line is result for the mixed dispersion media such as region S_1 of soil moisture 5% and region S_2 of soil moisture 10%, and blue dashed line is the result for mixed dispersion media 5% and 20%. From in Fig.4(b), we can see the following features:

(1)The responses from soil surface of mixed dispersion media for 5% and 10% are same as result of 5%. But, the responses from different dispersion media and perfect conductor can see the effect of both dispersion media and normalized distance.

(2)The responses from soil surface of two dispersion media for 5% and 20% are bigger than that of another media. As a reason, we can understand as influence of dispersion media with soil moisture 20% such as equivalent permittivity.

IV. CONCLUSION

In this paper, we proposed a method for deciding the parameters to satisfy the experiment values, and also checked the effectiveness of this method, based on the Kramers-Kronig relation. We also investigated the influence of pulse responses for the dry density of gray San Antonio clay loam using the medium constants which can be found by proposed method.

REFERENCES

[1] M. Nishimoto, S. Ueno, and K. Nagayoshi, "Classification of Shallowly Buried Objects Using Ground Penetrating Radar", The papers of Tech. on Electromagnetic Theory, IEE Japan, EMT-05-17, pp.21-25, 2005.(in Japanese)

[2] M. Sato, "Subsurface Imaging by Ground Penetrating Radar", IEICE Trans. Electron., vol.J85-C, no.7, pp.520-530, 2002.

[3] T. Tanaka and T. Takenaka, "FDTD Analysis of Time Domain Inverse Problem for Cylindrical Underground Objects", Proc. Society Conf. of IEICE, C-1-29, 1999.(in Japanese)

[4] J. E. Hipp, "Soil Electromagnetic Parameters as Functions of Frequency, Soil Density, and Soil Moisture", Proc. IEEE, vol.62, no.1, pp.98-103, Jan. 1974.

[5] T. Hosono, "Meta-Electromagnetics", Morikita, 1999. (in Japanese)

[6] T. Hosono, "Fundamental of Linear Black Box", Corona-Sha, 1980. (in Japanese)

[7] Z. Szabo, G. H. Park, R. Hedge, and E. P. Li, "A Unique Extraction of Metamaterial Parameters based on Kramers-Kronig Relationship", IEEE Trans. Microwave Theory Tech., vol.58, no.10, pp.2646-2653, 2010.

[8] T. Hosono, "Numerical inversion of Laplace transform and some applications to wave optics", Radio Science, vol.16, no.6, pp.1015-1019, 1981.

[9] T. Hosono, International Series of Monographs on Advanced Electromagnetics; FILT, vol.2, Science House Inc., Oct., 2013.

[10] R. Ozaki, N. Sugizaki, and T. Yamasaki: "Numerical Analysis of Pulse Responses in the Dispersion Media", IEICE Trans. Electron., vol.E97-C, no.1, 2014.